Published in final edited form as:
Neuroreport. 2009 February 18; 20(3): 257–262. doi:10.1097/WNR.0b013e3283200111.

T-type calcium channels regulate cortical plasticity in-vivo

Victor N. Uebele[a], **Cindy E. Nuss**[a], **Vincent P. Santarelli**[a], **Susan L. Garson**[a], **James C. Barrow**[b], **Shaun R. Stauffer**[b], **Kenneth S. Koblan**[a], **John J. Renger**[a], **Sara Aton**[c], **Julie Seibt**[c], **Michelle Dumoulin**[c], **Sushil K. Jha**[c], **Tammi Coleman**[c], and **Marcos G. Frank**[c]

[a] Department of Sleep Research, University of Pennsylvania, Philadelphia, Pennsylvania, USA

[b] Department of Medicinal Chemistry, Merck Research Laboratories, University of Pennsylvania, Philadelphia, Pennsylvania, USA

[c] Department of Neuroscience, School of Medicine, University of Pennsylvania, Philadelphia, Pennsylvania, USA

Abstract

T-type voltage-dependent calcium channels may play an important role in synaptic plasticity, but lack of specific antagonists has hampered investigation into this possible function. We investigated the role of the T-type channel in a canonical model of in-vivo cortical plasticity triggered by monocular deprivation. We identified a compound (TTA-I1) with subnanomolar potency in standard voltage clamp assays and high selectivity for the T-type channel. When infused intracortically, TTA-I1 reduced cortical plasticity triggered by monocular deprivation while preserving normal visual response properties. These results show that the T-type calcium channel plays a central role in cortical plasticity.

Keywords

Cav3.3; CavT; Kir2.3; LVA; monocular deprivation; ocular dominance; synaptic remodeling; voltage-gated

Introduction

T-type calcium channels are unusual members of the voltage-dependent class of calcium channels (VDCCs). Unlike most VDCCs that allow extracellular calcium into neurons after activation by membrane depolarization (e.g. high-voltage activated), T types are inactivated at resting membrane potentials and become ‘de-inactivated’ only after a period of membrane hyperpolarization. Small depolarizations then open the channel giving rise to a calcium-mediated low-threshold spike that drives burst firing in neurons [1].

The function of the T-type channel is not completely understood, but it may be important in synaptic plasticity. T-type channels are enriched in the neocortex and thalamus and are highly concentrated in dendrites [1]. They may also mediate several types of in-vitro plasticity [2]. The precise contribution of T-type channels to synaptic plasticity is, however, unclear because available antagonists inhibit other VDCCs or strongly influence other ion channels [3].

We investigated the role of the T-type channel in a classic model of cortical plasticity *in vivo*. Monocular deprivation (MD) during a critical period of development causes a rapid

Correspondence to Marcos G. Frank, PhD, Department of Neuroscience, School of Medicine, University of Pennsylvania, Philadelphia, PA-19104, USA, Tel: + 1 215 746 0388; fax: + 1 215 573 9050; mgf@mail.med.upenn.edu.

remodeling of the visual cortex in favor of the nondeprived eye; a process known as ocular dominance plasticity [4]. We determined the effects of selective T-type channel antagonism on ocular dominance plasticity by infusing the visual cortex with a newly identified T-type antagonist with subnanomolar potency (TTA-I1).

Methods

In-vitro identification and screening of a novel T-type antagonist

An in-vitro screening protocol [5] identified a potent T-type antagonist (TTA-I1), *N*-(4-fluorobenzyl)-1-{3-[5-(1H-1,2,4-triazol-1-ylmethyl)-1H-indol-3-yl]propyl}-*N*-(2,2,2-trifluoroethyl)piperidin-4-amine [5–7]. We then tested TTA-I1 for functional inhibition of CACNA1G, CACNA1H, CACNA1C [8], CACNA1A, CACNA1B, and CACNA1E calcium channels [9], as well as an array of additional targets in functional and binding assays at MDS Pharma Services according to standard protocols (http://www.mdsps.com). Assuming off target activity would most likely occur at other ion channels, targets were chosen on the basis of available ion channel assays.

Electrophysiological verification

Whole-cell patch-clamp recordings on HEK-293 cells expressing human CACNA1G, CACNA1H, CACNA1I, or CACNA1C calcium channels [8] were carried out at room temperature. Currents were recorded and analyzed using equipment and software similar to that described earlier [8]. To record T-type calcium currents, patch pipettes contained (in mM) 125 CsCl, 10 TEA-Cl, 10 HEPES, 8 NaCl, 0.06 $CaCl_2$, 0.6 EGTA, 4 Mg-ATP, 0.3 GTP, and pH was adjusted to 7.2 with CsOH. The extracellular solution was (in mM): 130 NaCl, 4 KCl, 30 glucose, 20 HEPES, 1 $MgCl_2$, 2 $CaCl_2$, and pH adjusted to 7.4 with NaOH. Baseline T-type calcium currents were elicited by depolarizing from holding to −20 mV for 70 ms, cycling every 10 s from a holding potential of −100 mV and every 20 s from a holding potential of −80 mV.

CACNA1C currents were recorded using internal solution (in mM) 135 CsCl, 10 EGTA, 10 HEPES, 1 $MgCl_2$, 5 Mg-ATP, 0.1 GTP, pH 7.2 (CsOH) and external solution (in mM) 150 Choline-Cl, 15 $BaCl_2$, 1 $MgCl_2$, 10 HEPES, 5 TEA-OH, pH 7.2 (TEA-OH). Cells were held at −90 mV and 100 ms test pulses to +10 mV were given every 3 s.

In-vivo procedures: minipump implantation and monocular deprivation

Nine cats were prepared for cranial surgeries during the critical period as described earlier [10]. A craniotomy was made over primary visual cortex and a 30-gauge cannula (Durect Corporation, Cupertino California, USA) was positioned in the visual cortex and anchored with two to three bone screws and dental acrylic. The cannula was attached to a 2ML2 Alzet osmotic minipump (Durect Corporation) placed subcutaneously. Each visual hemisphere was implanted with pumps either delivering vehicle (n=4, 50% DMSO, 50% artificial cerebrospinal fluid) or 5 μM (n=1) or 50 μM (n=4) TTA-I1 in vehicle. The pumps were presoaked in warm, sterile saline before surgery to ensure that infusion began immediately after implantation (pumping rate: 5 μl/h; pump duration: 14–16 days). All cats were treated with antibiotics and analgesics [10]. Once the animals had recovered, they were returned to their home cages for up to 11 days at which time they were anesthetized with isoflorane gas and had one eye sutured shut. They were again returned to their cages and the eye remained closed for 2–3 days [11]. Five cats of comparable age (mean ± SEM: 35.8 ± 1.46 days), but with no MD were also analyzed to provide normative comparison data (data from three cats reproduced with permission from Jha *et al.* [10]).

Microelectrode recordings in visual cortex

The nine cats undergoing MD and the normally sighted cats were prepared for microelectrode recordings and analyses as described earlier [10]. After the assignment of ocular dominance ranks for each neuron, scalar measures of plasticity and visual response properties (orientation selectivity, signal-to-noise) were calculated [10,12]. Three vehicles and two TTA-I1 hemispheres were excluded from analyses because the infusion tubing was damaged. Parametric data were assessed with one-way analyses of variance (ANOVAs), nonparametric data were assessed with nonparametric ANOVAs (Kruskal–Wallis or Friedman on ranks); significant main effects were further evaluated with Student–Newman–Keuls (SNK) post-hoc tests.

Additional in-vivo control experiments

To determine whether TTA-I1 by itself disrupted visual processing in normally sighted animals, two additional cats were implanted with minipumps containing either 50 μM TTA-I1 (placed in the right visual cortex) or vehicle (placed in the left visual cortex). At the end of the infusion period, the cats were prepared for microelectrode recording of visual responses (age at assay: 38 and 39 days). After an initial sampling of single neuronal responses in the TTA-I1-infused hemispheres, we examined the acute effects of TTA-I1 in the vehicle-infused hemispheres using protocols comparable to those used by previous investigators [13]. Visual response properties were computed and analyzed using a repeated-measure ANOVA for nonparametric data, followed by SNK post-hoc tests where appropriate. All animal procedures were approved by animal care (Institutional Animal Care and Use) committee of the University of Pennsylvania.

Results

In-vitro screening of TTA-I1

The results of our in-vitro screening and testing of TTA-I1 are shown in Fig. 1 and Table 1. Current clamp measurements showed a resting membrane potential of approximately −20 mV, consistent with HEK 293 cells (data not shown). This suggests that most channels are in the inactivated state and any calcium flux is from the fraction of channels oscillating through the open state (Fig. 1a). The observed signal reflects calcium flux through the channel because the signal is dependent on tetracycline-induced expression, is independent of osmotic effects and the magnitude of the signal is dependent on the calcium concentration gradient between the wash solution and stimulus conditions.

The fluorescent imaging plate reader (FLIPR) assay identified TTA-I1 as a T-type antagonist with a potency of 31.9 nM (n=60). As a reference standard, the potency of mibefradil was 127.4 nM (n=3; Fig. 1b), consistent with reported values in similar assays [14,15]. These potency values, derived from a fit to all data, differ from the average potencies determined from independent runs by less than 10%. The state-dependent properties of TTA-I1 were characterized by voltage-clamp assays (Fig. 1c). Comparison of potencies determined at membrane holding potentials of −80 and −100 mV confirmed that TTA-I1 is a state-independent antagonist with potencies of 0.7 and 0.8 nM, respectively. Similar experiments with cells expressing CACNA1G (0.4 and 1.4 nM) and CACNA1H (3 and 2 nM) showed that TTA-I1 is a pan-T-type antagonist (data not shown).

Several additional assays showed that TTA-I1 had minimal antagonist activity at other calcium or ion channels. FLIPR-based calcium flux assays (as described in Ref. [9]) showed the half maximal inhibitory concentration values greater than 10 μM for CACNA1A, CACNA1B, and CACNA1E channels. Standard voltage-clamp assays showed that TTA-I1 had greater than 12 000-fold selectivity for T-type over L-type calcium channels (Fig. 1d). TTA-I1 was further

screened in a panel of binding assays as summarized in Table 1, which also showed high selectivity for T-type calcium channels versus other ion channels.

The effects of TTA-I1 on ocular dominance plasticity

Electrophysiological recordings were made in 477 neurons from seven TTA-I1-infused hemispheres (mean ± SEM age at MD: 35.75 ± 1.93 days), 314 neurons from five vehicle hemispheres (37.25 ± 0.25 days), and 665 neurons from nine normal hemispheres (mean ± SEM age at assay: 36.57 ± 1.5 days). The mean ± SEM days of infusion (and MD) were: TTA-I1, 10 ± 0.41 (2.25 ± 0.25) and vehicle, 9 ± 0.82 (2.25 ± 0.25).

The results of our in-vivo measurements are shown in Fig. 2. TTA-I1 inhibited plasticity without producing abnormal visual response properties. A slight difference was found in the number of visually unresponsive neurons in TTA-I1 cortices (1.9%) relative to vehicle-infused cortices (0.6%), but no differences in orientation selectivity or signal-to-noise (deprived eye or nondeprived eye ANOVAs, NS) between the groups (data not shown). An elevation was observed in nondeprived eye firing in vehicle-infused neurons at the preferred orientation compared with TTA-I1 and normal (10.9 ± 1.6 vs. 5.1 ± 1, 6.2 ± 1.3 Hz: ANOVA, F=4.6, $P < 0.022$, SNK $P < 0.05$) but no differences in mean firing between TTA-I1 and normal (SNK, NS) or between the groups in deprived eye firing at the preferred orientation (ANOVA, NS).

Nonspecific effects of TTA-I1, chronic and acute measurements

TTA-I1 had no significant effects on peak-firing rates, orientation selectivity or signal-to-noise in visual cortical neurons from normally sighted cats (ANOVA, NS, data not shown). Scalar measures of ocular dominance in TTA-I1-infused hemispheres were also within normative values for cats with binocular vision (n=89 neurons, mean ± SEM CBI: 0.53 ± 0.14; MI: 0.38 ± 0.07, n=2).

Acute application of TTA-I1 also failed to significantly alter basic visual response properties, even after 30 min of continuous application (Fig. 2b and c). This was evaluated in nine visual cortical neurons (four from cat 1, five from cat 2). For example, TTA-I1 had no significant effects on orientation selectivity as shown in two representative neurons (Fig. 2b); nor were there any significant effects in any visual response property relative to vehicle in group means (repeated measure ANOVA, NS: all measures).

Discussion

We used a high-throughput FLIPR screen to identify a compound with subnanomolar potency and high selectivity for T-type channels. When infused intracortically, TTA-I1-reduced plasticity while leaving other neuronal response properties intact. The suppression of plasticity is not because of abnormalities in cortical function because TTA-I1 does not produce unresponsive cortex or gross alterations in visual responses as reported with other drugs [16]. TTA-I1 also had no significant effects on visual response properties either when combined with MD or in cats with normal binocular vision. Our results are also probably not caused by TTA-Il action at other VDCCs or other neurotransmitter receptors. TTA-I1 had greater than 12 000-fold selectivity for T-type over L-type calcium channels with negligible functional effect on other high-voltage activated calcium channels or displacement of radioligands for γ-aminobutyric acid (GABA) and glutamate receptors at micromolar concentrations *in vitro*. Micromolar concentrations of TTA-I1 inhibited binding to K_A, K_V, hERG potassium channels and the 5-HT1 receptor to varying degrees (Table 1). The concentration of an agent used in in-vitro assays, however, must be scaled up by several orders of magnitude to maintain equivalent concentrations *in vivo* [16]. Therefore, milli-molar concentrations of TTA-I1 would be required to produce comparable inhibition of these channels and receptors *in vivo*. Nor can our results

be ascribed to partial 5-HT1 antagonism, because intracortical infusion of a broad spectrum 5-HT1 antagonist does not inhibit ocular dominance plasticity [17].

A most likely explanation of our results is that T-type channels influence cortical plasticity by altering neuronal excitability and/or by providing a calcium signal necessary for synaptic remodeling. T-type channels are enriched in dendrites [18] where they modulate burst discharges and the propagation of excitation from distal to proximal neuronal sites [1,19]. Depending on their dendritic concentration, they may gate levels of calcium sufficient to trigger either long-term potentiation or long-term depression [1,19] and possibly gene transcription [20,21]. In addition, T-type channels are located in GABAergic cells [18], subsets of which are critical for ocular dominance plasticity [22]. If present in these subtypes, they may powerfully modulate GABAergic input onto pyramidal neurons. A final intriguing possibility is that T-type channels may regulate sleep-dependent changes in cortical circuits. Sleep enhances ocular dominance plasticity through unknown activity-dependent mechanisms [10]. The kinetics of the T-type channel make it an especially attractive candidate source of extracellular calcium during slow-wave sleep as this brain state is characterized by sustained neuronal hyperpolarization and low-threshold spike-mediated oscillations [23].

Conclusion

The function of T-type calcium channels in the central nervous system is unknown. We now show that these VDCCs may play a critical role in synaptic plasticity.

Acknowledgments

This study was supported by departmental funds from the University of Pennsylvania, PHS 5-R01-MH067568 and Merck Research Laboratories.

References

1. Yunker AMR, McEnery MW. Low-voltage-activated (‘T-Type’) calcium channels in review. J Bioenerg Biomembr 2003;35:533–575. [PubMed: 15000520]
2. Komatsu Y, Iwakiri M. Low-threshold Ca^{2+} channels mediate induction of long-term potentiation in kitten visual cortex. J Neurophysiol 1992;67:401–410. [PubMed: 1349036]
3. Yunker AMR. Modulation and pharmacology of low voltage-activated (‘T-Type’) calcium channels. J Bioenerg Biomembr 2003;35:577–598. [PubMed: 15000521]
4. Hubel DH, Wiesel TN. The period of susceptibility to the physiological effects of unilateral eye closure in kittens. J Physiol 1970;206:419–436. [PubMed: 5498493]
5. Shipe WD, Barrow JC, Yang ZQ, Lindsley CW, Yang FV, Schlegel KA, et al. Design, synthesis and evaluation of a novel 4-aminomethyl-4-fluoropiperidine as a T-type Ca^{2+} channel antagonist. J Med Chem 2008;51:6471–6477. [PubMed: 18817368]
6. Baker, R.; Bourrain, S.; Castro, P.; Jose, L.; Chambers, MS.; Guiblin, AR., et al. Preparation of azolylindoles and analogs as 5-HT1D alpha receptor agonists. PCT Int Appl. WO9604274A1. 1996.
7. Russell MG, Matassa VG, Pengilley RP, Van Niel MB, Sohal B, Watt AP, et al. 3-[3-(Piperidin-1-yl) propyl]indoles as highly selective h5-HT1D receptor agonists. J Med Chem 1999;42:4981–5001. [PubMed: 10585208]
8. Xia M, Imredy JP, Koblan KS, Bennett P, Connolly TM. State-dependent inhibition of L-type calcium channels: cell-based assay in high-throughput format. Anal Biochem 2004;327:74–81. [PubMed: 15033513]
9. Dai G, Haedo RJ, Warren VA, Ratliff KS, Bugianesi RM, Rush A, et al. A high-throughput assay for evaluating state dependence and subtype selectivity of Cav2 calcium channel inhibitors. Assay Drug Dev Technol 2008;6:195–212. [PubMed: 18471074]
10. Jha SK, Jones BE, Coleman T, Steinmetz N, Law C, Griffin G, et al. Sleep-dependent plasticity requires cortical activity. J Neurosci 2005;25:9266–9274. [PubMed: 16207886]

11. Crair MC, Ruthazer ES, Gillespie DC, Stryker MP. Relationship between the ocular dominance and orientation maps in visual cortex of monocularly deprived cats. Neuron 1997;19:307–318. [PubMed: 9292721]
12. Seibt J, Aton S, Jha SK, Dimoulin M, Coleman C, Frank MG. The non-benzodiazepine hypnotic Zolpidem impairs sleep-dependent cortical plasticity. Sleep 2008;31:1381–1392. [PubMed: 18853935]
13. Higley MJ, Contreras D. Cellular mechanisms of suppressive interactions between somatosensory responses In Vivo. J Neurophysiol 2007;97:647–658. [PubMed: 17065248]
14. Xia M, Imredy JP, Santarelli VP, Liang HA, Condra CL, Bennett P, et al. Generation and characterization of a cell line with inducible expression of Ca(v)3.2 (T-type) channels. Assay Drug Dev Technol 2003;1:637–645. [PubMed: 15090236]
15. Xie X, Van Deusen AL, Vitko I, Babu DA, Davies LA, Huynh N, et al. Validation of high throughput screening assays against three subtypes of Ca(v)3 T-type channels using molecular and pharmacologic approaches. Assay Drug Dev Technol 2007;5:191–203. [PubMed: 17477828]
16. Bear M, Kleinschmidt A, Gu Q, Singer W. Disruption of experience-dependent synaptic modifications in striate cortex by infusion of an NMDA receptor antagonist. J Neurosci 1990;10:909–925. [PubMed: 1969466]
17. Gu W, Singer W. Involvement of serotonin in developmental plasticity in kitten visual cortex. Eur J Neurosci 1994;7:1146–1153. [PubMed: 7582087]
18. Goldberg JH, Lacefield CO, Yuste R. Global dendritic calcium spikes in mouse layer 5 low threshold spiking interneurones: implications for control of pyramidal cell bursting. J Physiol (Lond) 2004;558:465–478. [PubMed: 15146046]
19. Perez-Reyes E. Molecular physiology of low-voltage-activated T-type calcium channels. Physiol Rev 2003;83:117–161. [PubMed: 12506128]
20. Sejnowski TJ, Destexhe A. Why do we sleep? Brain Res 2000;886:208–223. [PubMed: 11119697]
21. Benington JH, Frank MG. Cellular and molecular connections between sleep and synaptic plasticity. Prog Neurobiol 2003;69:77–101.
22. Hensch TK, Fagiolini M. Excitatory-inhibitory balance and critical period plasticity in developing visual cortex. Prog Brain Res 2005;147:115–124. [PubMed: 15581701]
23. Steriade, M. Brain electrical activity and sensory processing during waking and sleep states. In: Kryger, MH.; Roth, T.; Dement, WC., editors. Principles and Practice of Sleep Medicine. Philadelphia: Saunders; 2005. p. 101-119.

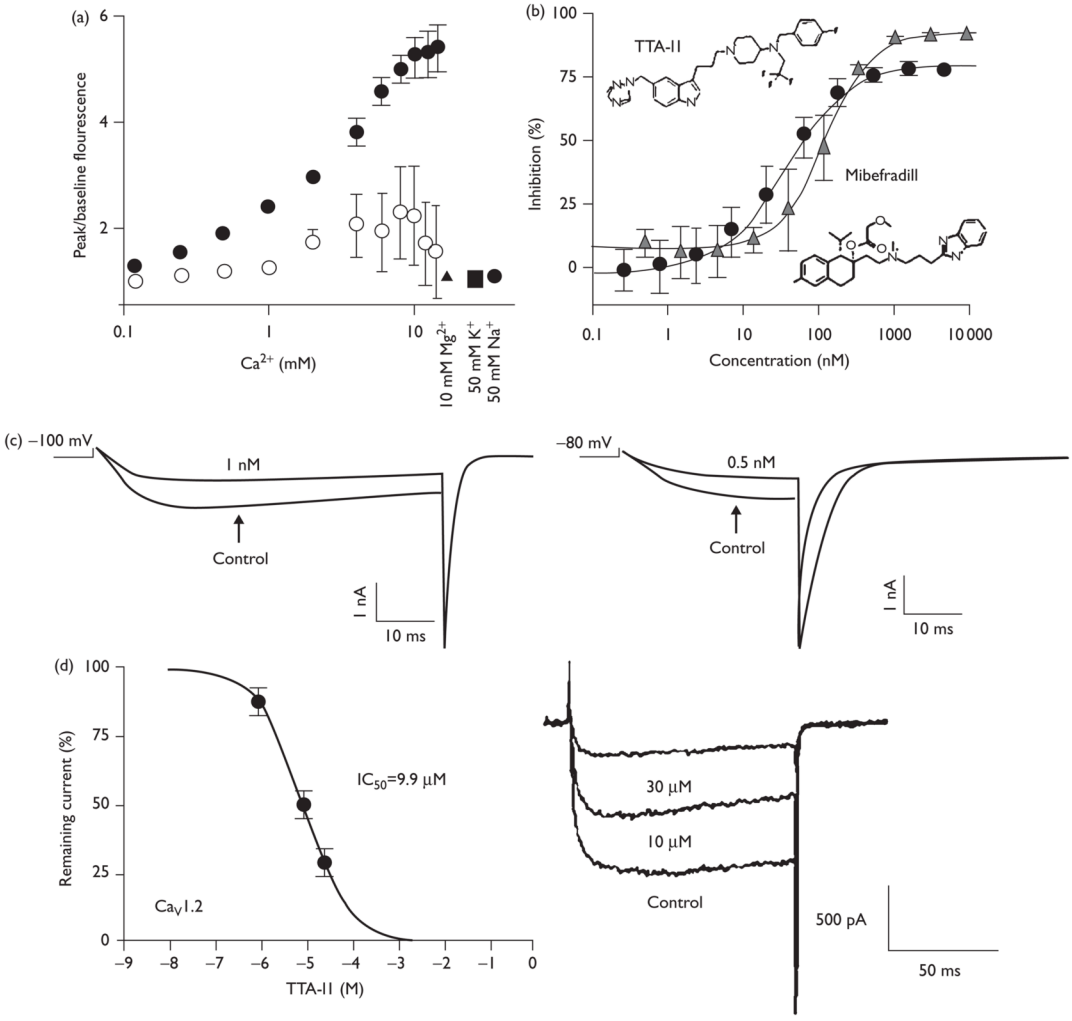

Fig. 1.

The T-type channel antagonist TTA-I1. (a) The fluorescence signal depends on channel expression and the calcium concentration gradient. Cells were plated and grown overnight in the absence (open circles) or presence (filled symbols) of tetracycline to induce CACNA1I expression. Signal was elicited by adding various concentrations of calcium, 10 mM Mg^{2+} (filled triangle), 50 mM K^+ (filled square) or 50 mM Na^+ (filled hexagon). Fluorescent signal is reported as a fold-increase over baseline. Values shown are mean ± SD. (b) Concentration-inhibition curves are plotted for TTA-I1 (black circles) and mibefradil (gray triangles). Values plotted are mean ± SD. (c) CACNA1I current tracings in the absence and presence of TTA-I1. Currents were elicited by depolarizations from a holding potential of −100 mV (left, 1.0 nM TTA-I1) or −80 mV (right, 0.5 nM TTA-I1). (d) CACNA1C current tracings at 0, 10 and 30 μM TTA-1I elicited from a holding potential of −90 mV.

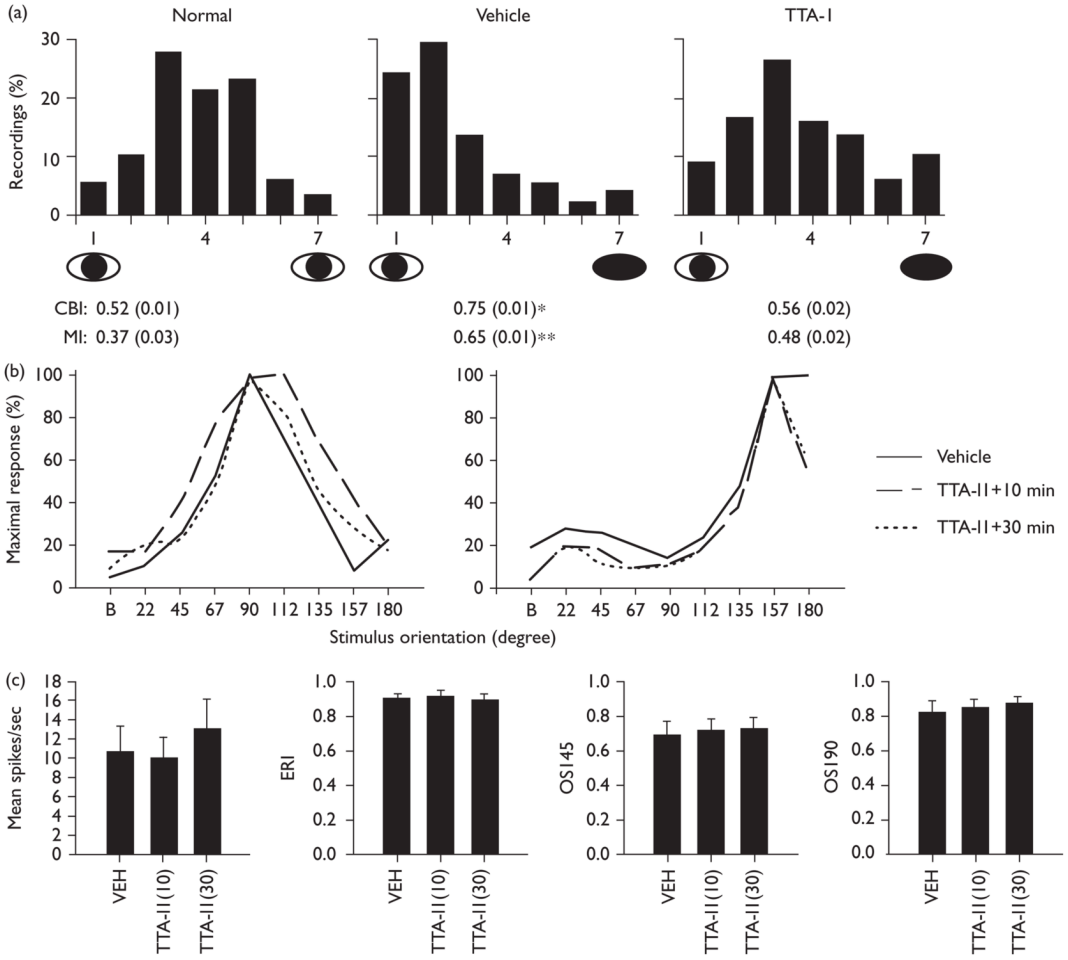

Fig. 2.

TTA-I1 blocks ocular dominance plasticity without producing abnormal visual responses. (a) Single-neuron ocular dominance histograms. Microelectrode recordings are from pooled normal hemispheres (no-MD), MD+vehicle infusion, and MD+TTA-I1 infusion (data from 5 and 50 μM infusion experiments were equivalent and thus pooled). Histograms are ranked such that 1 represents cells exclusively driven by the non-deprived (left) eye, 7 represents cells driven exclusively by the deprived (right) eye and 4 represents cells that are driven equally by the two eyes. Values below are corresponding mean ± SEM CBI [ANOVA (ranks), $H = 11.98$, $P < 0.003$: * = vehicle vs. normal, vehicle vs. TTA-I1, $P < 0.05$ SNK] and MI indices [ANOVA (ranks), $H = 11.94$, $P < 0.003$: ** = vehicle vs. normal, $P < 0.05$, SNK, all other comparisons, NS]. (b) Orientation selectivity in two representative neurons from two separate experiments (cat 1 and cat 2) before and 10 and 30 min after continuous application of 50 μM TTA-I1; the x-axis denotes orientation of gratings ('B' = blank screen) and the y-axis firing rates at each presentation normalized to the peak response. (c) Visual response properties before and after TTA-I1 application (means ± SEMs: $n = 9$ neurons). The left-most panel shows mean firing at the preferred orientation. The evoked response index (ERI) is a measure of signal-to-noise (evoked vs. background firing) the orientation selectivity index (OSI) measures responses at the preferred orientation vs. orientations 45 or 90 degrees orthogonal. No significant differences relative to vehicle on any measure were observed.

Table 1

Activity in ion channel binding assays

Assay target	Target source	Radioligand	Radioligand (K_D)	TTA-I1[a]
N-type calcium channel	Wistar rat brain frontal lobe	10 pM ^{125}I-conotoxin	51 pM	1
GABA-A	Wistar rat brain (minus cerebellum)	1 nM ^{3}H-muscimol	3.8 nM	−6
GABA-B	Wistar rat brain	0.6 nM ^{3}H-CGP-54626	2.3 nM	−2
Glutamate, AMPA	Wistar rat cerebral cortex	5 nM ^{3}H-AMPA	18 nM	12
Glutamate, Kainate	Wistar Rat brain (minus cerebellum)	5 nM ^{3}H-kainic acid	12 nM	−2
Glutamate, NMDA	Wistar rat cerebral cortex	4 nM ^{3}H-TCP	8.4 nM	−5
Glycine	Wistar rat spinal cord	10 nM ^{3}H-strychnine	13 nM	7
K channel, KATP	Syrian hamster pancreatic beta cells HIT-T15	5 nM ^{3}H-glibenclamide	0.64 nM	−9
K channel, KA	Wistar rat cerebral cortex	10 pM ^{125}I-dendrotoxin	35 pM	31
K channel, KV	Wistar rat brain frontal lobe	10 nM ^{125}I-charybdotoxin	27 pM	IC_{50}=6.6 μM
K channel, herg	Human recombinant, HEK-293 cells	50 pM ^{35}S-MK-499	1 nM	IC_{50}=0.3 μM

AMPA, α-amino-3-hydroxy-5-methyl-4-isoxazolepropionic acid; GABA, γ-aminobutyric acid; IC_{50}, half maximal inhibitory concentration.

[a] Values reported are percent inhibition at 10 μM. If inhibition was greater than 50%, a titration was run to determine IC_{50}.